A First Evaluation of Stereoscopic ERS-1 SAR Images: A Case Study in Southern Italy.

Viktor Kaufmann

Institute for Applied Geodesy and Photogrammetry
Graz University of Technology, Austria

presently
ESA/ESRIN, Frascati, Italy

Abstract

In order to investigate the potential of monoscopic and stereoscopic ERS-1 SAR images for geoscientific applications, such as geomorphological and topographic mapping, four test sites, from sea level to high mountains, have been set up in the region of Basilicata, Southern Italy.

This paper describes the first preliminary evaluation of a same-side ERS-1 SAR image stereopair in combination with its convergent stereo image partner in a hilly to mountaineous region which is characterized by denudational landforms. The SAR scenes were acquired in January and May, 1992 and were provided in digital format as SAR Precision Images (ground range images) with a picture element spacing of 12.5 x 12.5 m. As a first processing step the radar images were filtered to reduce the speckle noise. Several filters were applied and the results were assessed. In a case study a block of aerial photographs, a Landsat Thematic Mapper image and the three SAR Precision Images were evaluated in order to monitor the seasonal changes of the areal extent of a storage lake (Lake Monte Cotugno) in Southern Italy. Stereo viewing of the same-side stereo images gave a reasonable relief impression of the terrain (vertical exaggeration factor of 2.1) and was found to be very useful in image interpretation and for geomorphometrical measurements. One has to note that the relief impression is very much distorted because of forshortening and layover which limites the mapping possibilities. It was impossible to look stereoscopically at the ERS-1 SAR convergent stereo images obtained from crossing orbits.

Keywords: ERS-1, synthetic aperture radar, image interpretation, SAR filtering, same-side stereo, convergent stereo.

Paper presented at the 2nd International Symposium on High Mountain Remote Sensing Cartography, August 17 - 31, 1992, Beijing and Lhasa, P.R. of China.

1. Introduction

1.1 The first year for the ERS-1 satellite of ESA

On July 17, 1992 the first European Remote-Sensing Satellite (ERS-1) of the European Space Agency (ESA) was put in a sun-synchronous, near polar orbit with an Ariane 4 launcher. The ERS-1 mission objectives as described by Duchossois, 1991 are to study various environmental processes, mainly oceanographic as well as terrestrial. The ERS-1 satellite flies several instruments in order to achieve its mission objectives. The ERS-1 satellite and its payload are described in the ESA Bulletin No. 65, 1991. During only 12 months, ERS-1 has acquired raw data corresponding to 160.000 high-resolution images of the earth surface.

The Synthetic-Aperture Radar (SAR) of ERS-1

For land applications the Active Microwave Instrument (AMI) of ERS-1 which incorporates a Synthetic-Aperture Radar (SAR) is of main interest. The SAR works in the C-band (5.26 GHz frequency or 5.66 cm wavelength) with VV polarization. The imaging geometry is defined by the satellites nominal flying height of 785 km and nominal incidence angle at mid-swath of 23°. A full SAR scene covers an area of 100 by 100 km. The swath stand-off is 250 km to the right side of the orbital track. The spatial resolution is 25 m in ground range and 22 m in azimuth direction, respectively (Laur and Doherty, 1992). This may differ from the actual picture element (pixel) spacing of the ERS-1 SAR image products.

The various ERS-1 SAR products which can be ordered through the world-wide commercial distribution network (Eurimage, Radarsat International and Spot Image) are described in the ERS-1 User Handbook, 1992. The Fast Delivery Image, the Precision Image, the Ellipsoid Geocoded Image and the Terrain Geocoded Image, in digital or photographic format, are of main relevance for land application oriented projects.

Further details about the products can be found in the following ESA documents: ERS-1 Product Specifications, 1991 and ERS-1 Ground Station Product Specifications for Users, 1991.

1.2 Some pre-requisites

The radar backscatter (tonal information in the image) depends mainly on physical (slope, morphology, roughness, inhomogeneities, etc.) and electrical (dielectric constant, absorption, conductivity, i.e. moisture) characteristics of the surface, the near subsurface, and the surface cover (Elachi, 1988, p. 11). Radar imaging is neither limited by weather conditions nor by daytime.

1.3 Location of the test site

The area of interest is located in the region of Basilicata, Southern Italy at 40° 10′ N latitude and 15°20′ E longitude (Figure 1 und 2). It covers an area of approximately 13 x 13 km. See also Figure 3 which shows an ERS-1 radar stereogram covering the test site.
Some years ago a huge earth dam was built in the Sinni valley to dam up the water of the Sinni river. In the dry season of the year the water of Lake Monte Cotugno is used for irrigation of agricultural land. The water level of the reservoir changes significantly throughout the year

due to filling and discharge. The climate is mediterranean.
VEZZANI, 1967 describes the setting of the geological Sant' Arcangelo Basin, where the test site is located at. The region is very much affected my landsliding and soil erosion. The landscape is of badland geomorphology type.

1.4.1 Data used

1.4.1 Satellite images and aerial photographs

For the purpose of this study two different sources of satellite data had been used: Three ERS-1 SAR Precision Images (Figure 2) and one Landsat Thematic Mapper (TM) image.
The January ERS-1 image was acquired during a 3-day repeat cycle (ice) phase, and the other two images during a 35-day repeat cycle (multi-disciplinary) phase. The Landsat image (path 188, row 32) dates from August 11, 1991.
The subsets covering the test site are 1024 x 1024 pixels for the ERS-1 SAR 16-bit images and 512 x 512 for the Landsat TM image, respectively.
The test site is also covered by two strips of panchromatic photographs 1:37,000 taken on two different days (June 25, and July 1, 1990).
Ground truth is available for the ERS-1 SAR image acquired on May 17, 1992.
The satellite image data was provided digitally on computer compatible tapes (CCTs). Digital image processing was done on a PC-based workstation connected to a VAX-computer with the commercial software ERDAS and in-house developed software.

All necessary information for the user about ERS-1 satellite orbit, ERS-1 SAR radiometry and geometry, such as state vectors of the orbit, geographical coordinates of the four image corners, incidence angles at near, mid and far range, can be obtained from the auxiliary files on the CCT.

1.4.2 Map information

The test site is covered by four topographic maps 1:25,000 from the national mapping authorities. These maps represent the situation of 1956. Since the maps have not been updated yet, they do not show the present situation at all: Lake Monte Cotugno and the new highway are missing. Further, a road map 1:200,000 (1984), a topographical map 1:100,000 (1963) and a geological map 1:100,000 (1970) of the area were used.

1.5 Objectives

The objective of the case study described in this paper is to show a procedure how to use ERS-1 SAR images for different tasks, such as map updating, change detection of the areal extent of lakes and deriving qualitative and quantitative geomorphometric information. Finally, the advantages and disadvantages of ERS-1 SAR data related to above mentioned subjects should be assessed.
At this early stage of evaluation of first results of ERS-1 SAR images, limited literature is available. Nevertheless some, quite promising results have already been published (LICHTENEGGER, 1992).

2. First evaluation of ERS-1 SAR images

2.1 Radiometric filtering of ERS-1 SAR data

The visual perception and also the computerized analysis of SAR image data is complicated by radar speckle which is inherent to all radar images.
The theoretical background to understand radar speckle can be found in the textbook written by Ulaby and Dobson, 1989. Physical and mathematical models exist in order to describe radar speckle, which is, by the way, caused by phase-interference of the coherent radar signals from randomly distributed small scatterers within a resolution cell of the radar. Fully developed speckle has the character of multiplicative noise (Lopes et al., 1990 a). Based upon these models, several SAR speckle noise filtering algorithms have been developed. A summary of the most common SAR filters can be found in HOLECZ, 1989 and in NEZRY et al., 1991.

The histograms and also the cumulative ones of the three ERS-1 SAR image subsets are plotted in Figures 4a and 4b. We recognize that the histograms (Figure 4a) are not Gaussian shaped. Since ERS-1 SAR Precision Images are 3 looks amplitude images, the distribution should be the Chi distribution for stationary scenes and the K distribution for non stationary scenes (natural scenes with texture) (LOPES et al., 1990 a).
ERS-1 is the first remote sensing satellite which provides fully calibrated image data. Therefore we can compare the image statistics directly with each other. Figure 4a and 4b show that the radar backscatter on May 23, 1992 was higher than on the other two days. The presence of moisture in the surface, subsurface and vegetation is the reason for the increase in overall backscatter (see also Elachi, 1988, p. 207). Before May 23, 1992 there were several days with cloud cover and rainshowers all over Basilicata. The days before January 3 and May 17 were more or less cloudfree. This had been proved using NOAA AVHRR quicklooks.

Generally, a homogeneous region with fully developed speckle is statistically described only by one parameter, its mean value, which, in turn, is directly proportional to the backscattering coefficient. This implies for the proper filter process that we have to average digital counts within homogeneous regions, but on the other hand we should not average across bounderies and smooth out point and thin linear features. Several digital filters (Mean, Median, Edge Preserving Smoothing, Lee Sigma, Lee Local Statistics, Frost Minimum Mean Square, Li Adaptive Median and Gamma Maximum A Posteriori (MAP)) were implemented on the computer and applied on the SAR image from January, 3. In accordance with literature (Nezry, 1991) we found out that the adaptive filters, such as Frost and Lee, which take into account the local coefficient of variation, show quite good results. The well-known Frost filter was judged as one of the best. For example, the mean filter smoothes too much edges and bright spots, and therefore it is not an appropriate SAR image filter. Finally, all ERS-1 radar images were Frost filtered within a 5 x 5 window. The local coefficient of variation was determined with 0.30 within homogeneous regions of the radar images. The MAP filter (LOPES, 1990 b) is a very promising filter for further automatic image analysis and pattern recognition. We got the impression that the MAP filter smoothes too much in the homogeneous regions, at least for the given data and selected input parameters (Figure 5).

2.2 Three-dimensional viewing of ERS-1 SAR images

A first attempt was made to view at stereoscopic ERS-1 SAR image pairs with a pocket or mirror stereoscope. The anaglyph technique is also

applicable. The data may be presented in digital or in analog form. Hardcopies of the satellite images were produced with a Tektronix 46950DX printer in a comparatively low image quality.
The fundamentals of radar stereoscopy are reviewed by Leberl, 1990.
The vertical exaggeration in a radar stereo model is of main importance for a good stereo viewability. Exaggeration describes the "flatness" of the observed stereoscopic impression and is a function of the stereo-intersection angle.

2.2.1 Same-side ERS-1 SAR stereo

The same side ERS-1 SAR stereopair was oriented under the stereoscop properly by eliminating the vertical parallaxes. This is not only necessary for a comfortable stereo vision but also for a precise measurement of horizontal parallax differences. After a short period of adaption to the image speckle, the two SAR images could be fused to view a virtual three-dimensional model of the earth surface. Other test persons, not at all familiar with viewing through a stereoscope, had no problems to see the stereo model (see Figures 3 and 6a).
Using the exaggeration formula from Leberl, 1990, p. 322, we derived an exaggeration factor of 2.1 for the area near the earth dam of Lake Monte Cotugno.
At this stage we have to mention that the terrain is hilly to rugged. The lowest point is 170 m and the highest point 858 m above sea level.
Since the off nadir looking angle of ERS-1 SAR (17°15′ for the test site) is comperatively small, the image geometry is very much distorted. When looking at and analyzing radar images, we have to consider foreshortening, layover and shadow.
The basics of radargrammetry are also discussed by Leberl, 1990. Strobel, 1989 summaries the various possibilities of radar geometries for a given digital terrain model and a certain radar imaging geometry. As a result ERS-1 SAR images are very much affected by foreshortening and layover (compare Koopmans, 1983, pp. 226-227). Slopes facing the radar sensor appear in a very bright tone due to very high backscatter of the radar waves and are geometrically compressed, and back slopes on the other hand, are darker and stretched (Figures 6a and 6b).
We find layover in the SAR images of the test site. In mountaineous areas layover could be a limiting factor in stereoscopy. This has still to be proved in one of the mountaineous test sites located in Basilicata.

In general, radiometric differences between images were not to much, except for some agricultural fields and the water surface of Lake Monte Cotugno which shows higher backscatter because of the roughness of the water surface (Figure 5 and 7). Thus, the backscatter is mainly modulated by the topography of the terrain and wind action over water in the test site.

2.2.2 Convergent ERS-1 SAR stereo

For stereoscopic vision of an image stereopair some requirements have to be fulfiled, such as tone, texture, shape and size of objects should be within certain limits. When looking at Figure 6a and 6b, we recognize that length and grey tone of slopes shown in the ascending and descending images are more or less invers to each other. This means that a stereoscopic view of ERS-1 convergent stereos, explicitly those that are acquired at the cross-over of ascending and descending orbits, are not viewable, at least in hilly to mountainous areas at this latitude, even one tries to remap the grey values of one of the images

to fit the other image, as proposed in Leberl, 1990, p. 342-344.

2.3 Mapping of drainage pattern and topographic features

The intention of this task was to map drainage pattern, prominent ridges and other geomorphological and topographical features, such as the areal extent of the Lake Monte Cotugno, in order to study its feasibility and to get a dense network of control features for merging the geometries of the images with each other and with the map, respectively.
The results of the mapping process are presented in Figures 7a, 7b and 8.

It is very striking that in the ERS-1 SAR same-side stereopair all the small valleys and gullies, which can be seen in the aerial photographs, are clearly identifyable, mainly in the undulating hills in the north-west of the lake. Even in the monoscopic SAR image we can recognize valleys, gullies and mountain ridges to a great amount. By the way, a radar image should be viewed with its radar illumination direction towards the observer in order to get a orthoscopic relief impression (Figure 5).
The mapping of the drainage pattern in the Landsat TM false color composite was somehow difficult. But we identified sufficient features enough to correlate the TM image with the other data. The interpretation of the aerial photographs was done on the basis of an uncontrolled photo triangulation. The manuscript of the photointerpretation was finally reduced to fit the scale 1:64,000 (Figure 7a). All the mapping of the satellite data was performed in the scale 1:64.000. Therefore the Landsat image had to be resampled first from 30 m resolution to 25 m in order to derive the same scale as the radar images, which had been block averaged within a 2 x 2 window to retrieve 512 x 512 pixels with a 25 m spatial resolution.

2.4 Monitoring of Lake Monte Cotugno

As mentioned in subsection 1.4.2, Lake Monte Cotugno is not mapped in the old maps 1:25,000 and 1:100,000. Thus, it was obvious to update these maps with the existing information of previous mapping exercise. The map 1:100,000 was enlarged to the scale 1:64,000. The registration of all the data sets could be done without difficulties because there were sufficient control features, such as gullies draining into the lake and the earth dam, available. When overlaying the line drawings, the relief displacements in the SAR images got obvious (see Figure 7a and 7b). The mapping of the border line of the lake was easy in the aerial photographs and in the Landsat TM image, however, troublesome in the ERS-1 images.
The radar backscatter of a calm water surface is very low. Therefore, waterbodies appear as rather dark areas in the radar images. Wind induced waves encrease the radar backscatter significantly. Such wave patterns, which can also be seen along the shore line of the lake (Figure 6), make the discrimination of land and water to a difficult task. But we can overcome this problem by using collateral information, such as existing maps with contour lines, or even better a digital terrain model (DTM) when applying intelligent image segmentation and image analysis strategies, to clear out the ambiguities.
In case, we want to use ERS-1 SAR images only, multitemporal images are the proposed solution. Multitemporal ERS-1 images from the same orbit can be registered precisely, just by a translational shift of some few picture elements (see also Lichtenegger, 1992).
A larger arm of the lake, pointing north-west, is hardly recognizable,

not only because of the high backscatter of the wind induced waves but also because of its orientation parallel to the illumination direction.

Five individual manuscripts were combined to derive a change detection map (Figure 8).

Water mass balances can be calculated with known height information of the subsurface of the lake. This data could be gathered from the existing aerial photographs by means of a rigorous photogrammetric evaluation. At the time of acquisition of the aerial photographs the water level of the lake was very low, maybe, at the beginning of fillig up the reservoir.

2.5 Height and slope measurements

As an example, several height differences of distinct terrain points were measured in the ERS-1 same-side stereopair using a parallax bar and a mirror stereoscop. Also at this stage we have to mention that the radar hardcopies were of low quality and of course rasterized. Nevertheless, it was sufficient to perform some course measurements in the stereo images. Photographic products on film or paper would had been optimal for this purpose.
Three measurements of parallax differences were made for each point. By applying a simple parallax formula for computing height differences (Leberl, 1990), which is a course approximation of the ERS-1 SAR geometry, we obtained height differences with an accuracy of +/- 35 m.
Also slope length and inclination may be derived from similar measurements (Leberl, 1990) which is a little bit more troublesome, but feasible.

3. Conclusions and outlook

The first evaluation of ERS-1 SAR images showed promising results for geoscientific applications, especially for geomorphological mapping. Within the scope of this work we could demonstrate that the monitoring of inland water bodies, such as natural lakes or man-made reservoirs, is possible with ERS-1 radar images. This is due to the hortizontal water surface (stable radar geometry) and the rather low radar backscatter of a smooth water surface. Wind action may cause problems but can be handled with collateral information or with multitemporal SAR radar images. In high mountaineous regions layover may limit the use of this technique (mountains falling into the lake). But nevertheless, we have to consider the availability of remotely sensed data, for which ERS-1 SAR has advantages because of its all-weather capability.
Relief induced geometrical distortions are quite difficult to handle in a hilly to mountaineous area.
Moreover, a great potential has been identified in ERS-1 SAR interferometry which allows the evaluation of a high resolution digital terrain model from two radar images of close by orbits using the phase history of the radar signals. Besides this new approach, the conventional way of radargrammetric mapping in analog or digital form has still to be investigated. Combined ascending and descending ERS-1 SAR images in a geocoded mosaic could be also of further interest.

4. Acknowledgment

This research work had been carried out at ESRIN in Frascati, Italy. I am grateful to the Directorate of Observation of the Earth and its Environment of ESA, which had granted me a reseach fellowship for one

year. I have to thank very much Juerg Lichtenegger and Henry Laur, both of ESRIN, for their fruitful contributions to this work. Henry Laur provided the Gamma MAP filter, and the other SAR filter programs had been implemented by R.P. Dipak from the Asian Institute of Technology (AIT), Bangkok, Thailand. Dipak will publish his scientific results on ERS-1 SAR filtering in his forthcoming Ph.D. thesis.
The satellite data was provided by the Earthnet Programme Office, ESRIN. The support of the Istituto Geografico Militare (IGM), Florence, Italy, in selecting the aerial photographs is kindly appreciated.

5. References

G. DUCHOSSOIS, 1991, The ERS-1 Mission Objectives. ESA Bulletin, no. 65, pp. 16-25.

C. ELACHI, 1988, Spaceborne Radar Remote Sensing: Applications and Techniques. IEEE Press, Inc., New York, 255 p.

F. HOLECZ, 1989, A Study on Texture Measurements Applied to SAR Images. Final Report, Remote Sensing Laboratories, University of Zurich, Switzerland, 92 p.

B.N. KOOPMANNS, 1983, Spaceborne Imaging Radars, Present and Future. ITC Journal no. 3, pp. 223-231.

H. LAUR and G.M. DOHERTY, 1992, ERS-1 SAR Calibration. Proceedings of the ERS-1 Commissioning Phase, Final Review, April, 1992.

F.W. LEBERL, 1990, Radargrammetric Image Processing. Archtec House, Inc., 595 p.

J. LICHTENEGGER, 1992, ERS-1: Landuse Mapping and Crop Monitoring: A first close Look to SAR Data. Earth Observation Quarterly, nos. 37-38, ESA Publication Division, p. 1-5,

A. LOPES, H. LAUR and E. NEZRY, 1990 a, Statistical Distribution and Texture in Multilook and Complex SAR Images. Proceedings of IGARSS'90, pp. 2427-2430.

A. LOPES, E. NEZRY, R. TOUZI and H. LAUR, 1990 b, Maximum A Posteriori Speckle Filtering and First Order Texture Models in SAR Images. Proceedings of IGARSS'90, pp. 2409-2412.

E. NEZRY, A. LOPES and R. TOUZI, 1991, Detection of Structural and Textural Features for SAR Image Filtering. Proceedings of IGARSS'91, pp. 2169-2172.

D. STROBL, 1989, The Effects of Control Point Location Errors on SAR Geocoding in Mountainous Terrain. DIBAG Report No. 37, Graz Research Center, Austria, 113 p.

F.T. ULABY and M.C. DOBSON, 1989, Handbook of Radar Scattering Statistics for Terrain. Artech House, Inc., 357 p.

L. VEZZANI, 1967. Il bacino plio-pleistocenico di S. Arcangelo (Lucania), Atti Acc. Gioenia Sc. Nat. (Suppl. Sc. Geol.) s. VI, 18, pp. 207-227.

ESA Bulletin, 1991, no. 65, ERS-1 Special Issue. 130 p.

ERS-1 ESA PRODUCTS SPECIFICATIONS, 1991. ER-IS-GS-0501, ERSIN Earthnet Programme Office, 84 p.

ERS-1 GROUND STATIONS PRODUCTS SPECIFICATIONS FOR USERS, 1991. ER-IS-EPO-GS-0204, ESRIN Earthnet Programme Office, 97 p.

ERS-1 USER HANDBOOK, 1992. ESA SP-1148, ESA Publications Division, 159 p.

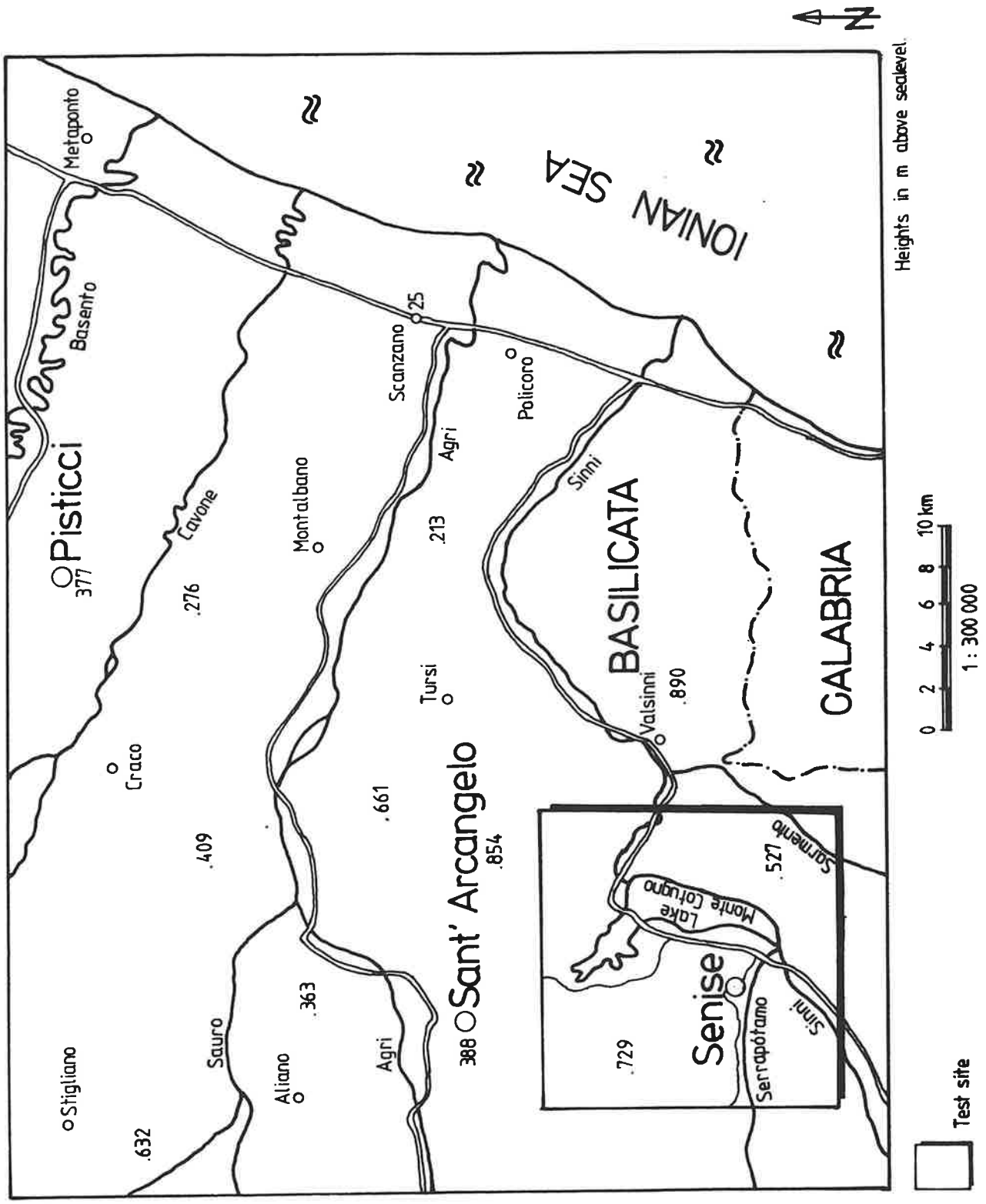

Figure 1: Location of the test site with Lake Monte Cotugno in the region of Basilicata, Southern Italy. The area is drained by the Sinni River.

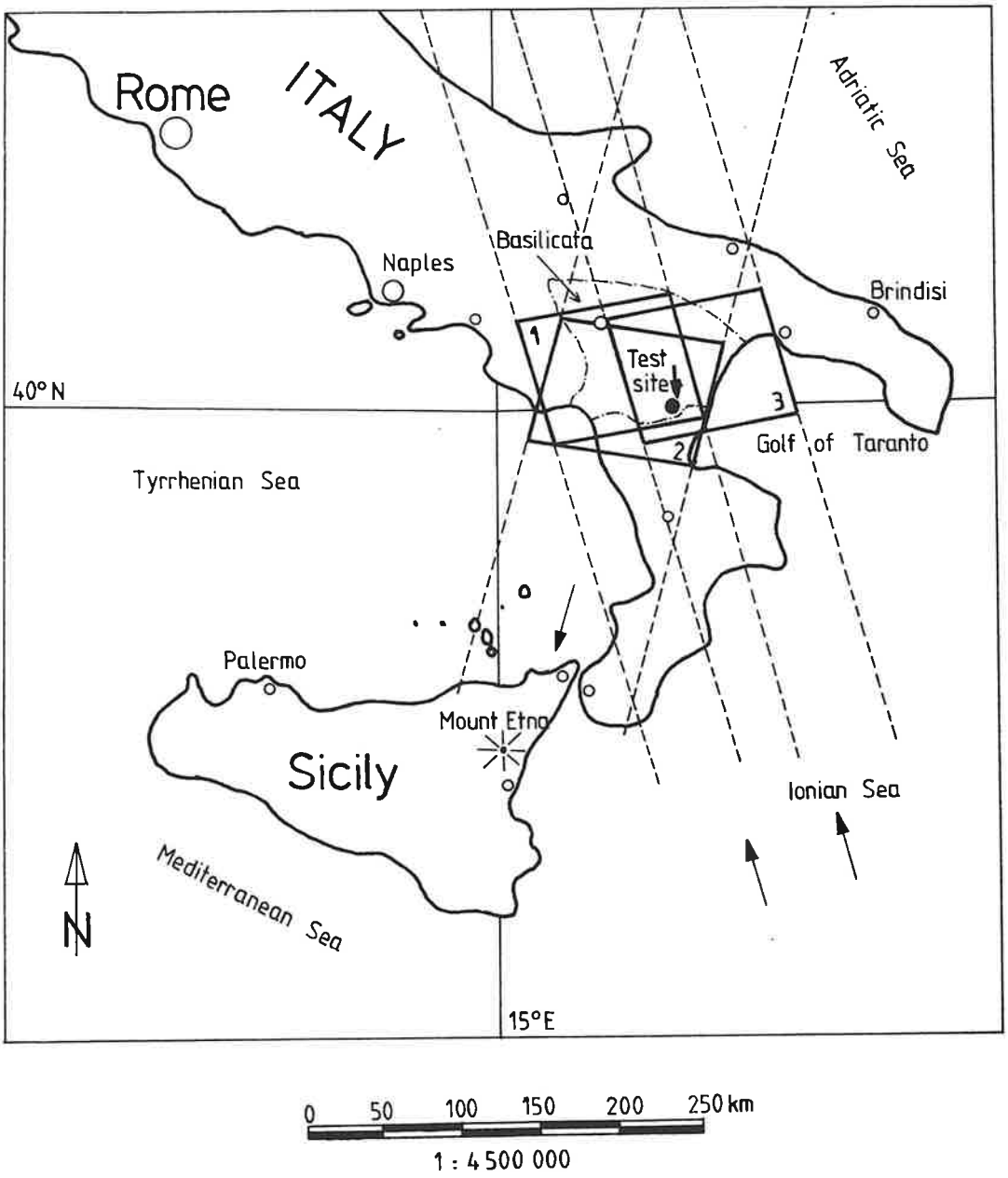

Figure 2: Coverage of the three ERS-1 SAR Precision Images over the test site The ERS-1 SAR tracks are indicated by dashed lines. Scene 1: Ascending orbit 2448 (frame 783) of January 3, 1992. Scene 2: Descending orbit 4375 (frame 2781) of May 17, 1992. Scene 3: Ascending orbit 4468, (frame 783) of May 23, 1992. Overpasses at 21:10:48, 09:40:44 and 21:08:31 UTC.

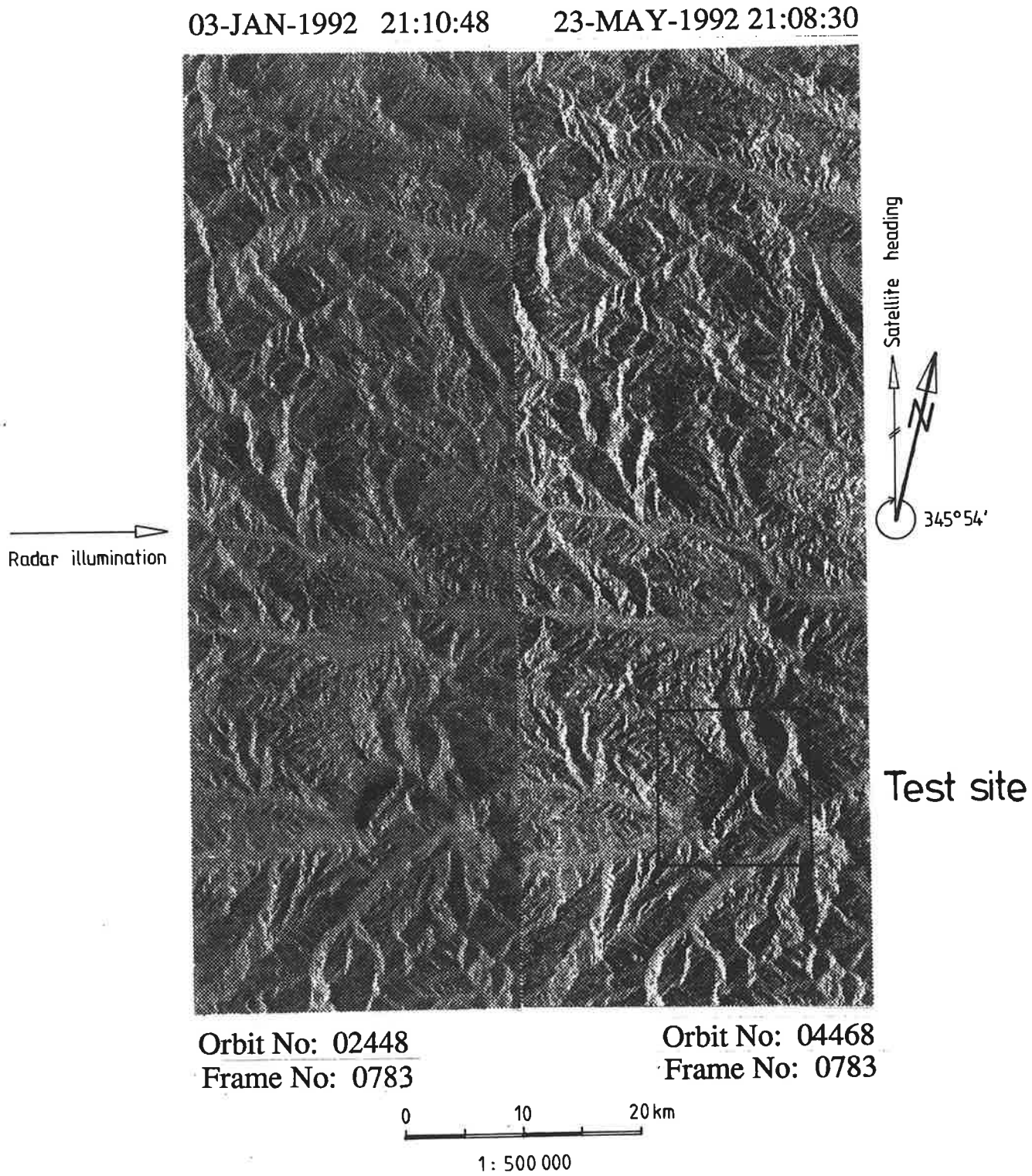

Figure 3: Stereogram composed of two ERS-1 SAR Precision Images taken from two adjacent ascending orbits. The base length of the same-side stereopair is 50.3 km. Incidence angles for both images are 25°14'37" and 21°28'47" near the earth dam. Therefore the stereo-intersection angle results in 3°45'50".

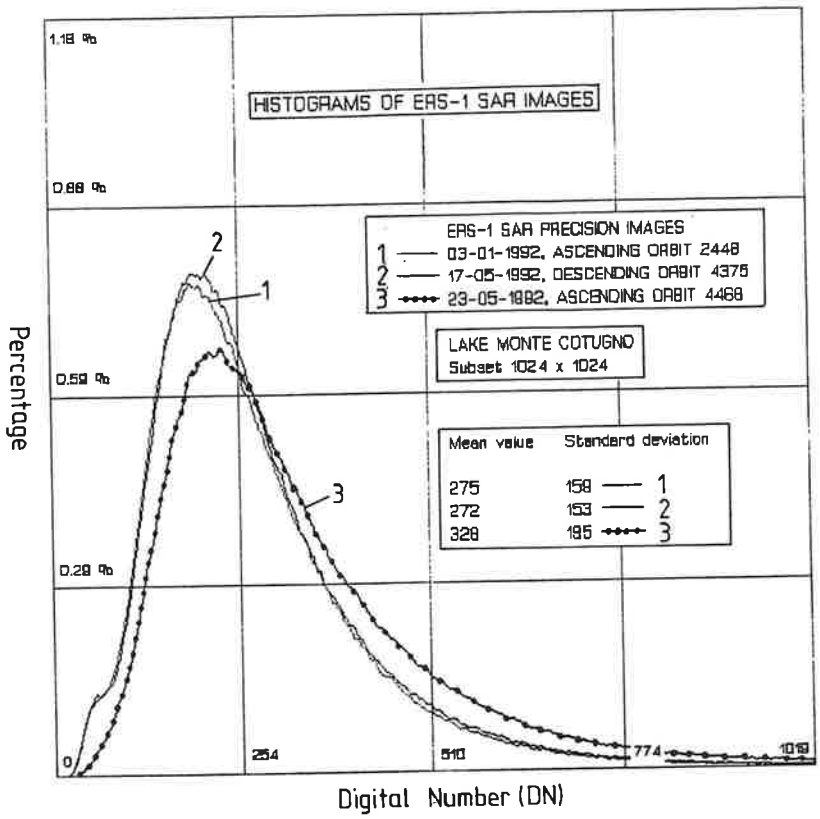

Figure 4a: Histograms of the three ERS-1 SAR Precision Images.

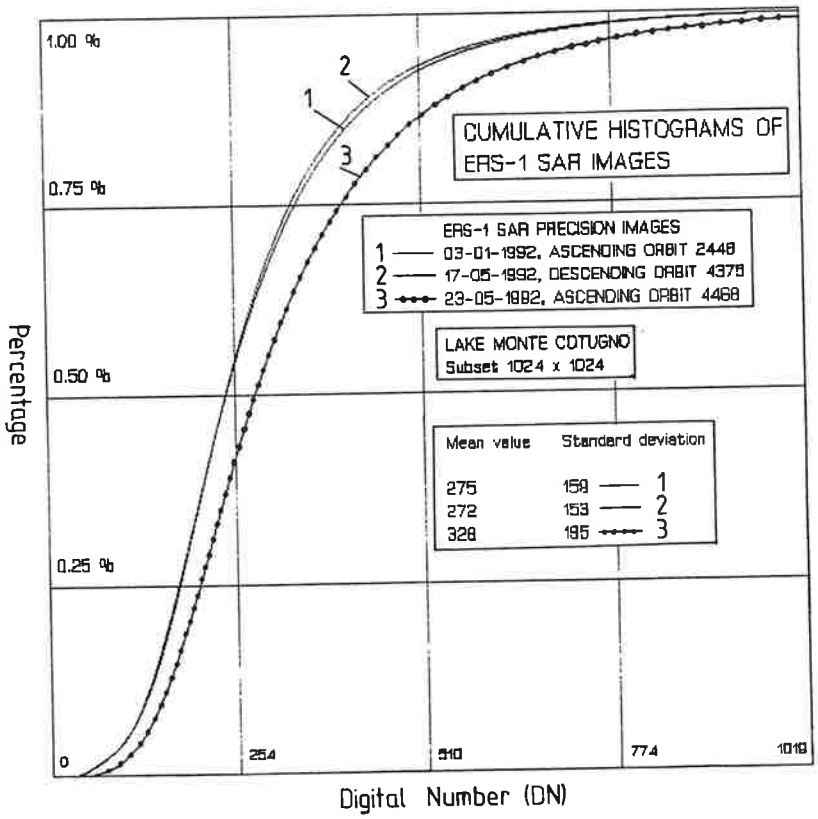

Figure 4b: Cumulative histograms.

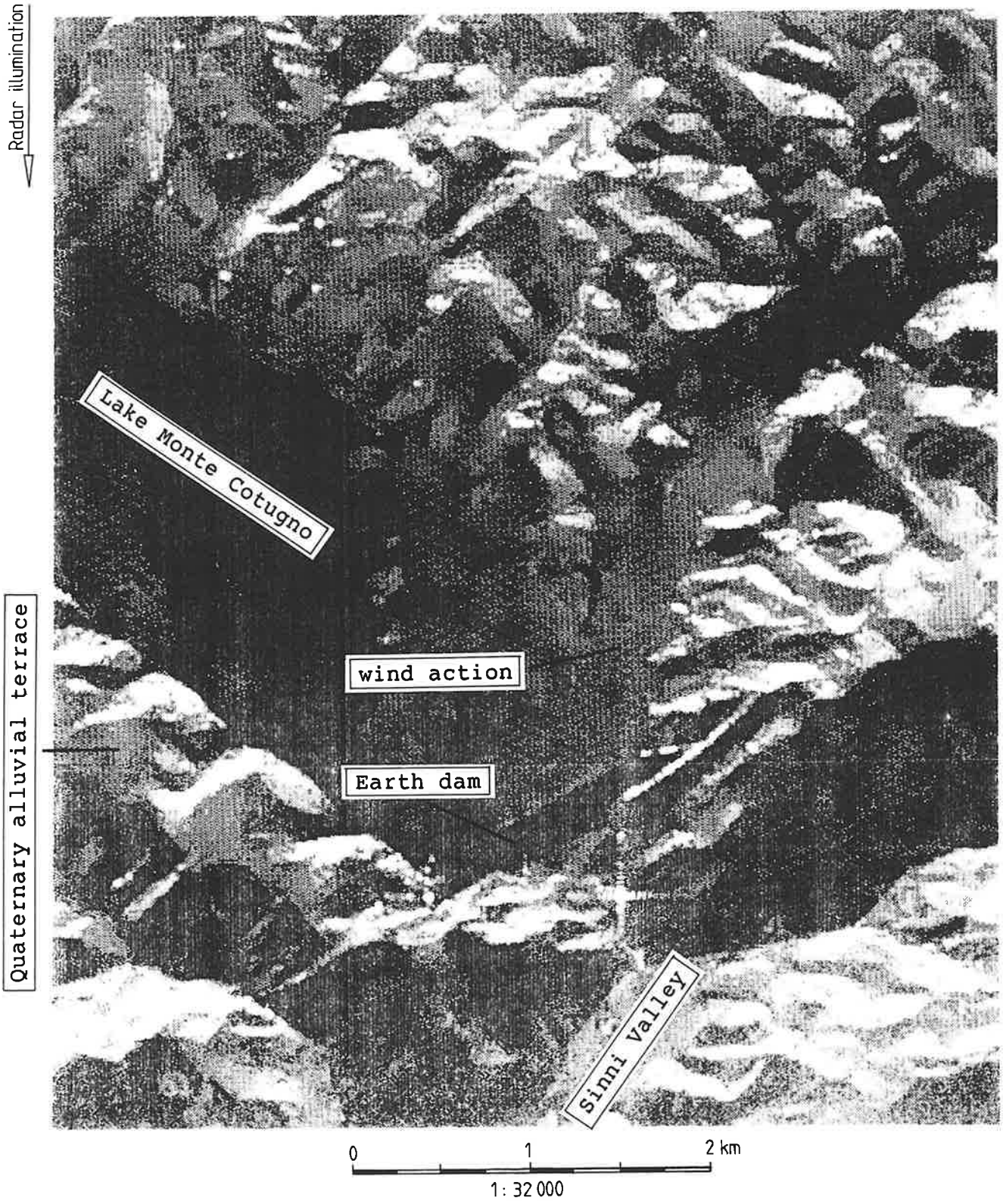

Figure 5: This subset (512 x 512 pixels) of the ERS-1 SAR image from January 3, 1992 had been filtered with the Maximum A Posteriori (MAP) approach. We recognize Lake Monte Cotugno with its mixture of calm and rough surface, the earth dam and a very bright response in the lower image part. A hollow cylindrical structure (15 m in diameter) acts as a corner reflector.

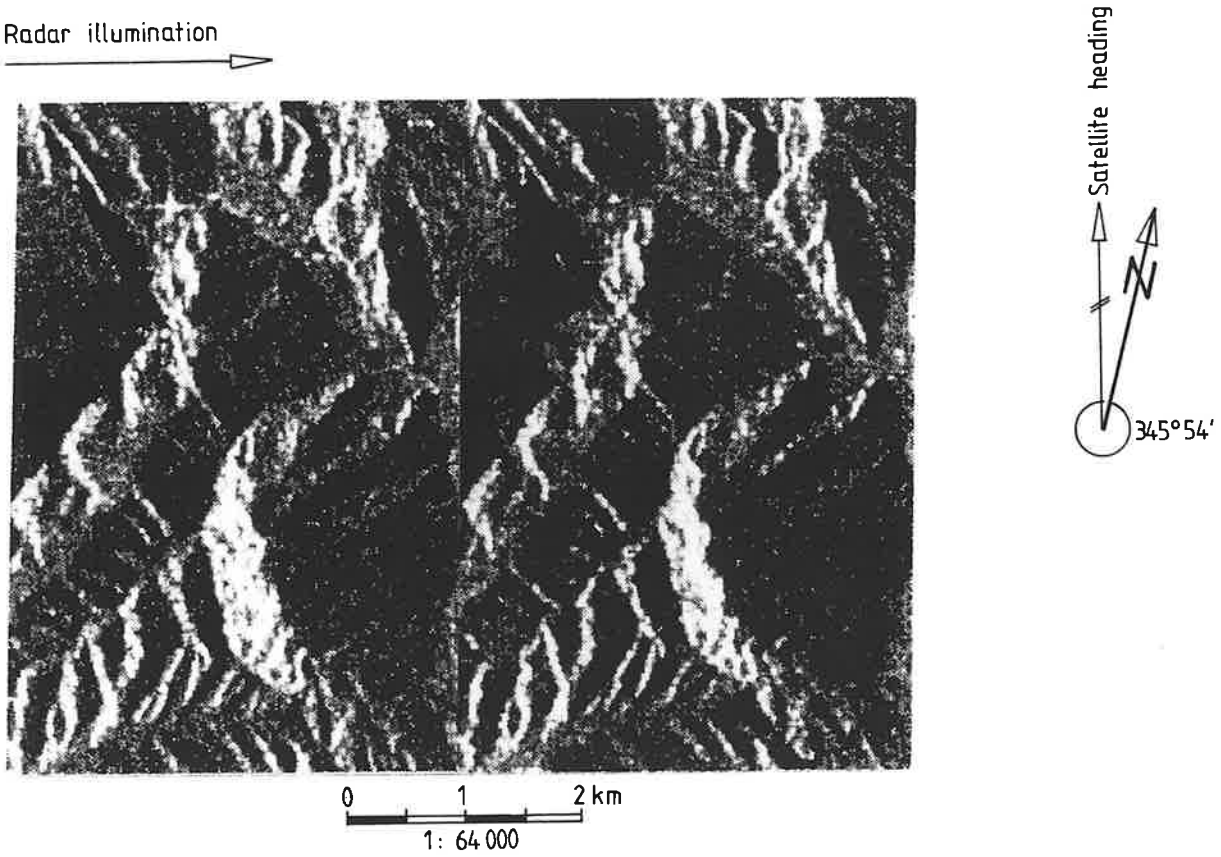

Figure 6a: This ERS-1 SAR stereogram shows part of Lake Monte Cotugno and the earth dam in left upper corner. The highest crests are 380 m above the valley floor.

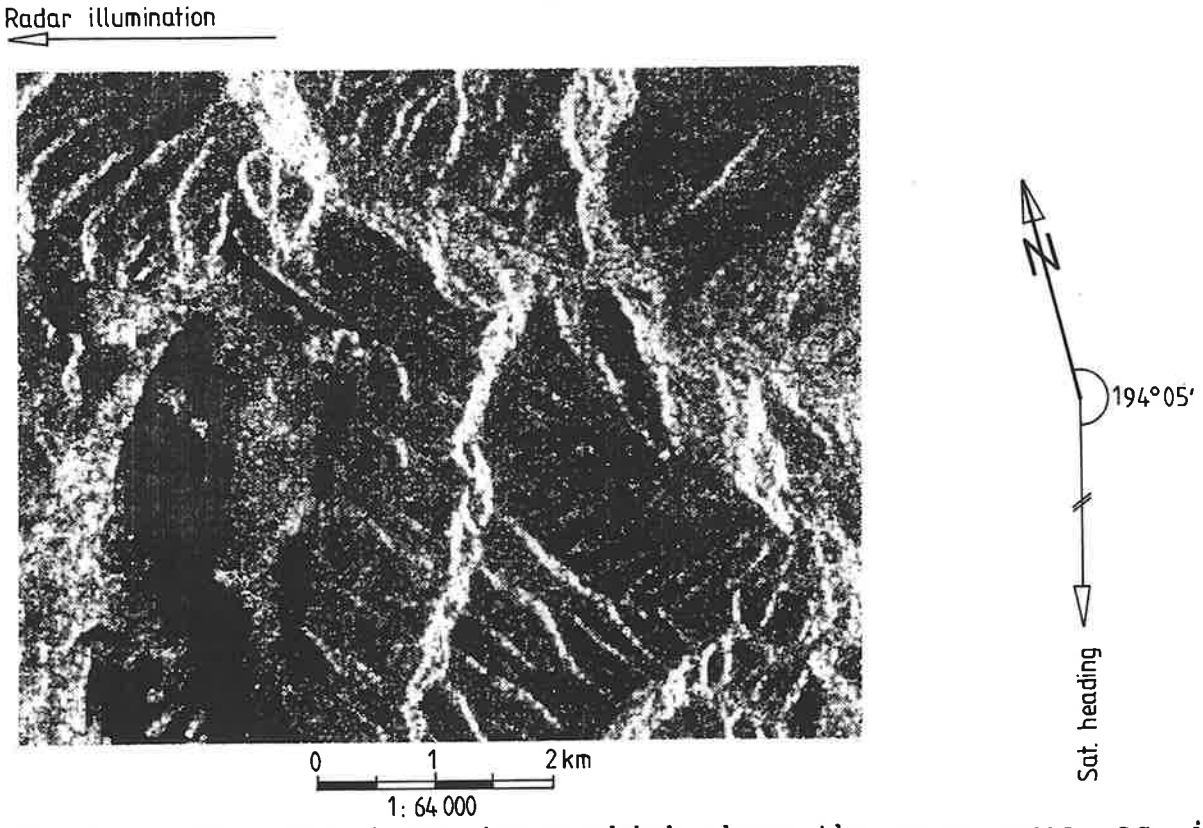

Figure 6b: Descending ERS-1 SAR image which shows the same area as in the stereogram above.

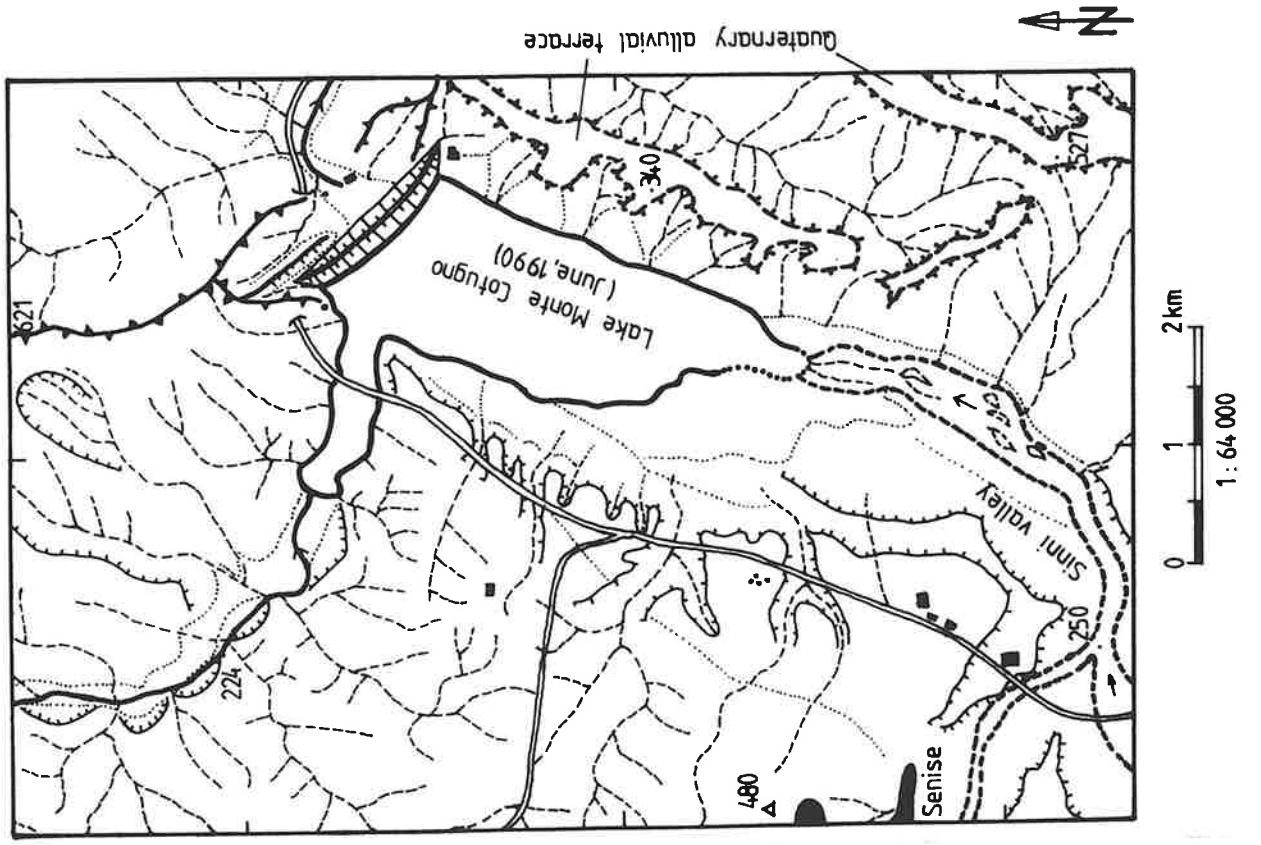

Figure 7a: Aerial photograph interpretation of the test site.

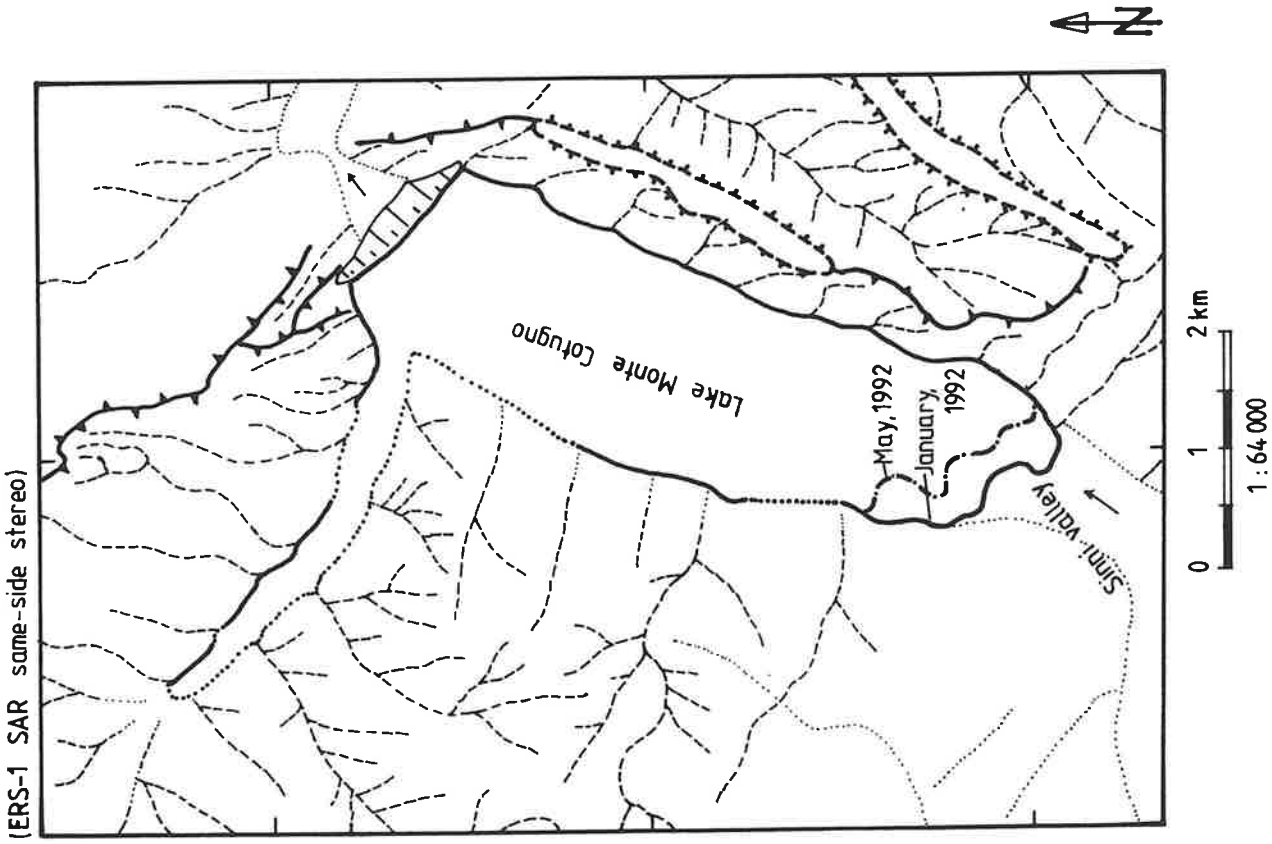

Figure 7b: ERS-1 SAR interpretation of the test site.

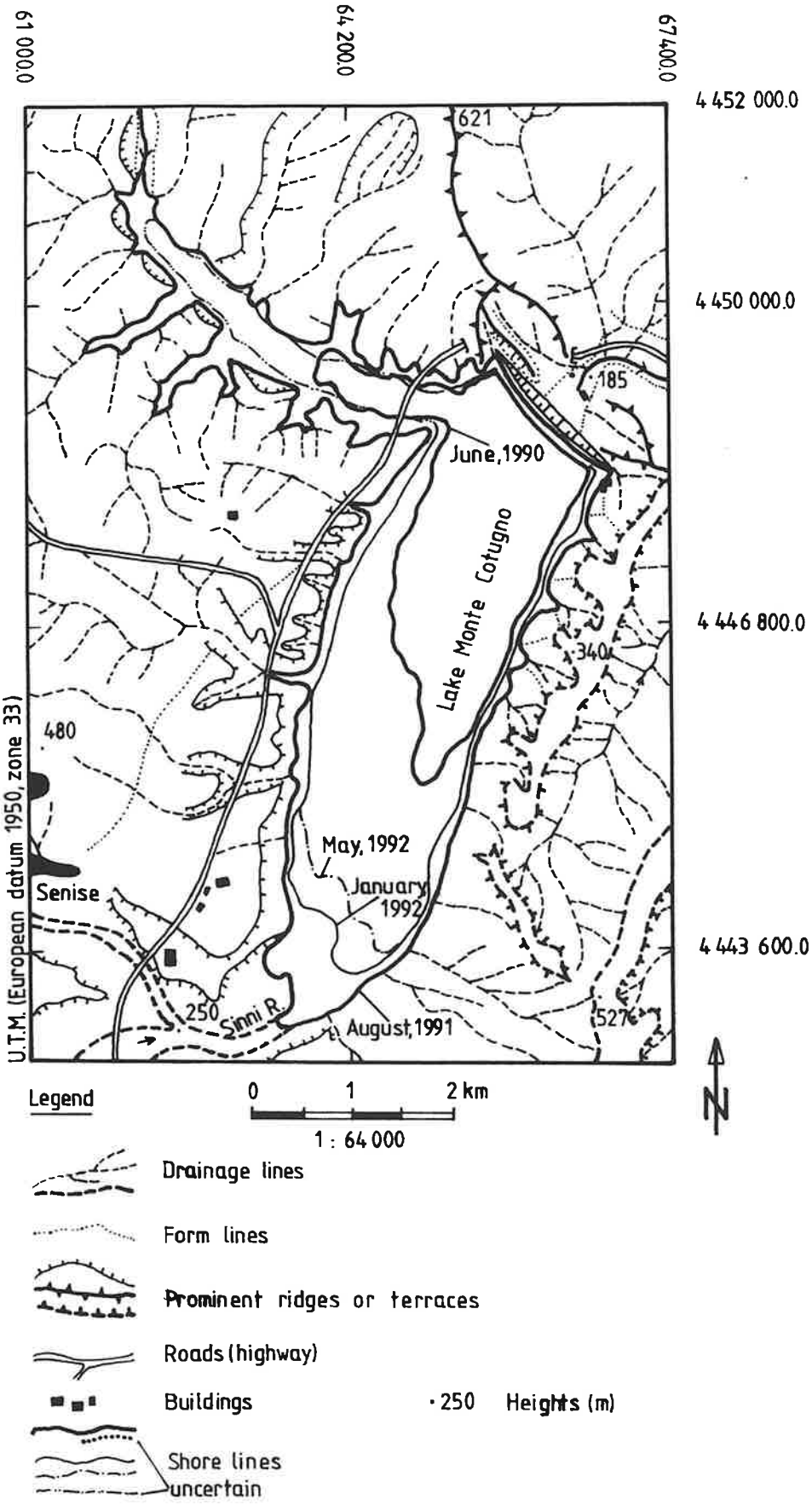

Figure 8: This map shows the changes of the areal extent of Lake Monte Cotugno as derived from multitemporal remotely sensed data.